

Altered expression and distribution of aquaporin-9 in the liver of rat with obstructive extrahepatic cholestasis

Giuseppe Calamita,¹ Domenico Ferri,² Patrizia Gena,¹ Flavia I. Carreras,³ Giuseppa E. Liquori,² Piero Portincasa,⁴ Raúl A. Marinelli,³ and Maria Svelto¹

¹Dipartimento di Fisiologia Generale ed Ambientale, ²Dipartimento di Zoologia, and ⁴Dipartimento di Medicina Interna e Medicina Pubblica, Università degli Studi di Bari, Bari, Italy; and ³Instituto de Fisiologia Experimental, Universidad Nacional de Rosario, Rosario, Argentina

Submitted 7 March 2008; accepted in final form 28 July 2008

Calamita G, Ferri D, Gena P, Carreras FI, Liquori GE, Portincasa P, Marinelli RA, Svelto M. Altered expression and distribution of aquaporin-9 in the liver of rat with obstructive extrahepatic cholestasis. *Am J Physiol Gastrointest Liver Physiol* 295: G682–G690, 2008. First published July 31, 2008; doi:10.1152/ajpgi.90226.2008.—Rat hepatocytes express aquaporin-9 (AQP9), a basolateral channel permeable to water, glycerol, and other small neutral solutes. Although liver AQP9 is known for mediating the uptake of sinusoidal blood glycerol, its relevance in bile secretion physiology and pathophysiology remains elusive. Here, we evaluated whether defective expression of AQP9 is associated to secretory dysfunction of rat hepatocytes following bile duct ligation (BDL). By immunoblotting, 1-day BDL resulted in a slight decrease of AQP9 protein in basolateral membranes and a simultaneous increase of AQP9 in intracellular membranes. This pattern was steadily accentuated in the subsequent days of BDL since at 7 days BDL basolateral membrane AQP9 decreased by 85% whereas intracellular AQP9 increased by 115%. However, the AQP9 immunoreactivity of the total liver membranes from day 7 of BDL rats was reduced by 49% compared with the sham counterpart. Results were confirmed by immunofluorescence and immunogold electron microscopy and consistent with biophysical studies showing considerable decrease of the basolateral membrane water and glycerol permeabilities of cholestatic hepatocytes. The AQP9 mRNA was slightly reduced only at day 7 of BDL, indicating that the dysregulation was mainly occurring at a posttranslational level. The altered expression of liver AQP9 during BDL was not dependent on insulin, a hormone known to negatively regulate AQP9 at a transcriptional level, since insulinemia was unchanged in 7-day BDL rats. Overall, these results suggest that extrahepatic cholestasis leads to downregulation of AQP9 in the hepatocyte basolateral plasma membrane and dysregulated aquaporin channels contribute to bile flow dysfunction of cholestatic hepatocyte.

aquaglyceroporin; water channel; bile; bile duct ligation

AQUAPORINS (AQPs) represent a widespread family of membrane channels that permeate only water (orthodox aquaporins) or small uncharged solutes such as glycerol in addition to water (aquaglyceroporins). AQPs have been found to be relevant to multiple physiological processes and diverse clinical dysfunctions (18). Rat hepatocytes express three AQP proteins: AQP8, 9, and 11 (see Ref. 37 for a review). AQP8 features multiple subcellular localizations being composed of an intracellular pool residing permanently in the hepatocyte smooth endoplasmic reticulum and mitochondria (8) and a choleric pool shuttling between cytoplasm (subapical vesicles) and canalic-

ular membrane under control of choleric stimuli (2, 10, 17). AQP9, an aquaglyceroporin of broad selectivity, resides exclusively on the basolateral membrane, where, during starvation, it is believed to mediate the uptake of gluconeogenic glycerol from portal bloodstream (3, 23, 38). AQP11 is an unusual AQP found in the endoplasmic reticulum (33) and whose water channel function is controversial (12, 46).

Bile secretion by hepatocytes involves the movement of water from portal bloodstream into bile canaliculus in response to transient osmotic gradients generated by active solute transport (31). Although evidence has been provided suggesting facilitation of osmotic water transport during canalicular bile secretion by apical AQP8 (17, 30), no direct information is currently available regarding the possible water channel function of hepatocyte AQP9 and its potential relevance to primary bile formation in health and disease.

Extrahepatic cholestasis is an abnormal condition characterized by biliary obstruction leading to reduction of bile flow and impairment of various transport mechanisms in both basolateral and canalicular membranes of hepatocytes (25). Dysregulation in the molecular expression of hepatocyte membrane transporters in obstructive cholestasis have been extensively investigated by using a model of bile duct ligation (BDL) in the rat. Interestingly, our recent work finding downregulated expression of hepatocyte AQP8 in BDL rats suggested pathophysiological relevance for liver AQPs in obstructive cholestasis (4). Thus the main purpose of this study was to determine the effect of BDL on the basolateral membrane osmotic water permeability and expression and subcellular distribution of AQP9 in rat liver.

MATERIALS AND METHODS

Animals and treatment. Adult male Wistar rats (250–300 g; 3 mo old; Harlan) were maintained on a standard diet and water ad libitum and housed in a temperature- and humidity-controlled environment under a constant 12:12-h light-dark cycle. Under ether anesthesia, the common bile duct was double ligated and cut between the ligatures. Control animals underwent a sham operation that consisted of exposure, but not ligation, of the common bile duct. After 1, 3, and 7 days of ligation, the animals were euthanized and livers were harvested for evaluation. Each experimental (BDL) or control (sham) group consisted of three to five rats. Dysregulated bile flow was verified by assaying the serum alkaline phosphatase activity and total bilirubin level as previously described (4). The protocol was conducted accord-

Address for reprint requests and other correspondence: G. Calamita, Dipartimento di Fisiologia Generale ed Ambientale, Università degli Studi di Bari, Via Amendola, 165/A, 70126 Bari, Italy (e-mail: calamita@biologia.uniba.it).

The costs of publication of this article were defrayed in part by the payment of page charges. The article must therefore be hereby marked “advertisement” in accordance with 18 U.S.C. Section 1734 solely to indicate this fact.

ing to the Guiding Principles for the Care and Use of Laboratory Animals.

Semiquantitative RT-PCR. Livers were removed from euthanized rats and frozen in liquid nitrogen. Total RNA from livers of sham operated or BDL rats was isolated by the TRIzol reagent (Invitrogen, San Diego, CA) following the manufacturer's protocol. The samples of total RNA were submitted to semiquantitative RT-PCR as previously described (2) by using the rat *AQP9* primers AQP9-start (5'-ATGCCTTCTGAGAAGGACGG-3') and AQP9-stop (5'-CTA-CATGATGACACTGAGCT-3'), which lead to the amplification of a 885-bp fragment of DNA. RT-PCR reactions were normalized against the β -actin expression (2).

Preparations of liver subcellular membrane fractions. Cholestatic and sham-operated livers were homogenized by 15 up-down strokes with a loose fitting Dounce homogenizer in four volumes of 0.3 M sucrose, containing 0.1 mM phenylmethylsulfonyl fluoride and 0.1 mM leupeptin (Sigma, St. Louis, MO). Total liver homogenates were subjected to low-speed centrifugation at 800 g for 10 min to obtain postnuclear supernatants and then subjected to centrifugation at 200,000 g for 60 min, yielding the total liver membrane fraction (10). Fractions enriched in total plasma membranes, basolateral membranes, or intracellular microsomal membranes were prepared from liver homogenates by differential centrifugation on discontinuous sucrose gradients as previously described (4, 10, 17). Proteins in plasma membrane fraction were assayed according to the method of Lowry (28). Enrichment and purity of plasma membranes were comparable to those reported previously (4, 30, 32).

Preparation of basolateral membrane vesicles and stopped-flow light scattering measurement of water and glycerol permeabilities. The basolateral membrane vesicles were prepared as previously described (30). The size of vesicles was determined with an N5 Submicron Particle Size Analyzer (Beckman Coulter, Palo Alto, CA) and by transmission electron microscopy. The time course of vesicle volume change was followed from changes in intensity of scattered light at the wavelength of 450 nm by using a Jasco FP-6200 (Jasco, Tokyo, Japan) stopped-flow reaction analyzer that has a 1.6-ms dead time and 99% mixing efficiency in <1 ms. Vesicle osmotic water permeability was measured by light scattering at 20°C as previously described (1). Briefly, 35 μ l of a concentrated vesicle suspension was diluted into 2.5 ml of a hypotonic (220 mosM) isolation medium (124 mM mannitol, 70 mM sucrose, 20 mM Tris·HCl, 1 mM EDTA and 5 mM EGTA, pH 7.4). One of the syringes of the stopped-flow apparatus was filled with the specimen suspension, whereas the other was filled with the same buffer to which mannitol was added to reach a final osmolarity of 500 mosM to establish a hypertonic gradient (140 mosM) upon mixing. The final protein concentration after mixing was of 100 μ g/ml. Immediately, after application of a hypertonic gradient, water outflow occurs, and the vesicles shrink, causing an increase in scattered light intensity. The data were fitted to a single exponential function and the related rate constant (K_i , s^{-1}) of the water efflux out of the analyzed specimen was measured. The osmotic water permeability coefficient (P_f), an index reflecting the osmotic water permeability of the vesicular membrane, was deduced from the K_i as described (42), using the equation:

$$P_f = K_i \cdot V_0 / A_v \cdot V_w \cdot \Delta C, \quad (1)$$

where K_i is the fitted exponential rate constant, V_0 is the initial mean vesicle volume, A_v is the mean vesicle surface, V_w is the molar volume of water, and ΔC is the osmotic gradient. The medium osmolarity was verified by a vapor-pressure osmometer (Wescor, Logan, UT).

For measurement of glycerol permeability, vesicles were subjected to a 150 mM inwardly directed gradient of glycerol as previously reported by Yang and coworkers (47). Glycerol permeability (P_{gly} ; cm/s) was computed by using the equation:

$$P_{gly} = 1/[(S/V)\tau] \quad (2)$$

where S/V is surface-to-volume ratio and τ is the exponential time constant fitted to the vesicle swelling phase of light scattering time course corresponding to glycerol entry.

Immunoblotting. Plasma membrane fractions were subjected to SDS-PAGE and transferred to polyvinyl difluoride membranes (NEN Life Science Products, Boston, MA). After blocking and washing, blots were incubated overnight at 4°C with rabbit affinity-purified antibodies against AQP9 (1 μ g/ml; Alpha Diagnostics International, San Antonio, TX) or for 2 h at room temperature (RT) with a 1:5,000 dilution of goat antibodies against Na^+K^+ -ATPase (Calbiochem-Novabiochem, La Jolla, CA). The blots were washed and then incubated for 1 h at RT with corresponding horseradish peroxidase-conjugated secondary antibodies. Protein bands were detected by enhanced chemiluminescence detection system (ECL, Amersham, Little Chalfont, UK). Autoradiographs were obtained by exposing the membranes to Kodak XAR films, and the bands were quantified by densitometry using Gel-Pro32 software (Gel-Pro Analyzer, Media Cybernetics, Silver Spring, MD).

Immunohistochemistry. Cholestatic and sham-operated rats were euthanized after ether anesthesia and their livers were quickly removed, sliced, and fixed overnight by immersion with 4% paraformaldehyde. For the immunoperoxidase light microscopy, samples of liver were quickly processed to be included in a hydrophilic resin (Technovit 8100, Heraeus-Kulzer, Wehrheim, Germany) and processed as previously reported (1). For the immunofluorescence experiments, after being washed the livers were incubated overnight in PBS with 30% sucrose added and were embedded in Optimal Cutting Temperature embedding medium (Bio-Optica, Milan, Italy). Frozen sections were cut to a thickness of 4 μ m. The sections were washed in PBS for 10 min and then blocked with PBS-gelatin 0.1% for 15 min at RT before being incubated with the rabbit affinity-purified antibodies against the rat AQP9 (3 μ g/ml) for 2 h at RT. Negative controls were performed by omitting the primary antibody. After three 5-min washes in PBS-gelatin 0.1%, the sections were incubated with FITC-conjugated goat anti-rabbit secondary antibody (Molecular Probes, Eugene, OR) for 1 h at RT. The sections were again washed one time in PBS added with NaCl 2.7% followed by two 10-min washes in PBS. The coverslips were mounted by using a mounting medium consisting of glycerol 50%, Tris·HCl 0.2 M, pH 8.0 and *n*-propyl gallate 2.5%. The section's fluorescence intensity was quantified and displayed graphically via a Leica DMRXA photomicroscope equipped with a CCD camera (Princeton Instruments, New York, NY).

Immunogold electron microscopy. Samples of liver were fixed in a mixture of 3% paraformaldehyde and 1% glutaraldehyde in 0.1 M PBS, at pH 7.4, for 4 h at 4°C. Some specimens were postfixed in 1% OsO_4 in PBS for 30 min at 4°C. Fixed specimens were dehydrated in ethanol then embedded in Epon (Taab, Reading, UK). For immunoelectron microscopy, ultrathin sections of osmicated samples were oxidized with sodium metaperiodate to restore specific labeling. Both osmicated and nonosmicated sections were treated with 0.05 M glycine in PBS buffer for 15 min at RT. Grids were incubated for 30 min at RT with 1% BSA in PBS containing 0.2% gelatin (PBG) and then placed on a drop of AQP9 antibodies (10 μ g/ml of PBG) overnight at 4°C. The grids were then incubated in 1:10 10-nm gold-conjugated anti-rabbit IgG (Sigma) in PBG for 1 h at RT and lightly stained with uranyl acetate and lead citrate. Finally, the grids were observed with a Zeiss EM 109 electron microscope. Immunolabeling controls were performed as in immunofluorescence.

Statistical analysis. Experiments with each group of animals were performed at least in triplicate. Means \pm SE were calculated based on three to five independent preparations. Data were analyzed statistically by the Student's *t*-test. Results were considered statistically significant when $P < 0.05$.

RESULTS

Ligation of the common bile duct resulted in extrahepatic cholestasis, as indicated by the increased serum levels of total bilirubin and alkaline phosphatase. Levels of total serum bilirubin increased to 6.7 ± 0.7 mg/dl (sham-operated rats, 0.6 ± 0.2 mg/dl) and serum alkaline phosphatase to $1,093 \pm 184$ U/l (sham-operated rats, 434 ± 57 U/l) at *day 7* after BDL.

Effect of BDL on AQP9 mRNA expression. Semiquantitative RT-PCR analysis was performed to study the effect of BDL on AQP9 mRNA expression. Compared with sham-operated controls, levels of AQP9 mRNA were unchanged on *day 1* and *3* of BDL but slightly decreased (-35%) on *day 7* BDL (Fig. 1, A and B). The AQP9 mRNA expression was normalized against that of the housekeeper gene β -actin (Fig. 1A).

Effect of BDL on AQP9 protein expression and subcellular distribution. Immunoblotting with liver total, plasma, and intracellular membrane fractions was performed to evaluate the effect of BDL on AQP9 protein expression and subcellular localization. One-day BDL did not affect the plasma membrane expression of AQP9 whereas a 25% reduction was seen at *day 3* of BDL. After 7 days of BDL, there was a remarkable reduction of basolateral membrane AQP9 (-85%) (Fig. 2, A and D). The

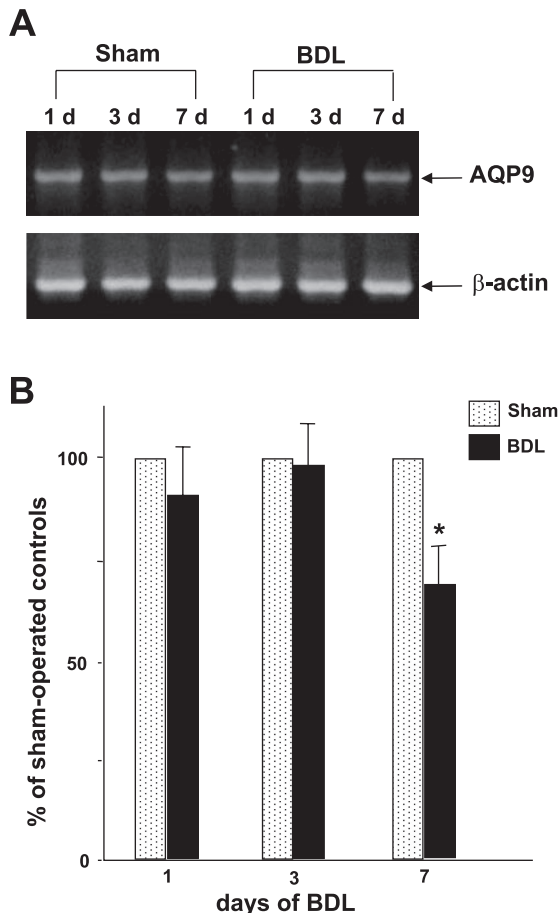


Fig. 1. Effect of bile duct ligation (BDL) on the expression of the AQP9 mRNA in rat liver. A: RT-PCR analysis, representative gel. The expression of AQP9 (885-bp band, top) is normalized against that of the housekeeper gene β -actin (509 bp band, bottom). B: densitometric analysis of hepatic AQP9 mRNA expression. The expression of AQP9 in sham rats is arbitrarily normalized to 100%. * $P < 0.05$. d, Days.

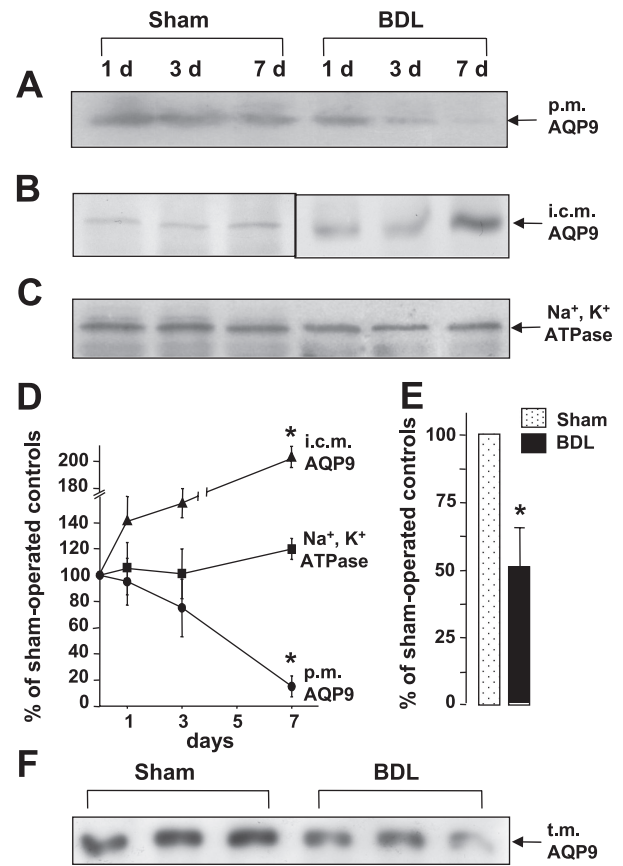


Fig. 2. Effect of BDL on the subcellular distribution of AQP9 protein. A–C and F: representative immunoblots for AQP9 (32 kDa; A, B, F) and plasma membrane $\text{Na}^+\text{-K}^+$ -adenosine triphosphatase ($\text{Na}^+\text{-K}^+$ -ATPase) (110 kDa corresponding to the α_1 subunit; C). D and E: densitometric analyses ($n = 3$) represented as time course (D) and histograms (total membranes at *day 7*; E). Data (means \pm SE) are expressed as percentage of sham-operated controls. ●, plasma membrane (p.m.) AQP9; ▲, intracellular membrane (i.c.m.) AQP9; ■, p.m. $\text{Na}^+\text{-K}^+$ -ATPase; total membrane AQP9 (t.m. AQP9). * $P < 0.05$.

AQP9 protein expression was compared with that of the $\text{Na}^+\text{-K}^+$ -adenosine triphosphatase (α_1 subunit) (Fig. 2, C and D), a plasma membrane protein remaining unaltered during BDL (11). Of note, the immunolabeling of the intracellular membrane fraction increased steadily from *day 1* BDL and became remarkable at *day 7* BDL ($+115\%$), whereas the weak intracellular immunoreactivity to AQP9 did not change in the sham livers. Overall, the AQP9 immunoreactivity detected in the total liver membrane fraction from *day 7* of BDL rats was reduced by 49% ($P < 0.01$) compared with the sham counterpart (Fig. 2, E and F). This finding suggests that the basolateral membrane insertion of AQP9 in cholestatic hepatocytes is impaired and the overall liver AQP9 protein is considerably reduced after 7 days of BDL (Fig. 2, B and D). BDL did not alter the yield of total membrane proteins (data not shown). The downregulation of basolateral AQP9 was not due to insulin, a hormone exerting a negative effect on the expression of liver AQP9 (23), since 7 days of BDL did not change the insulinemia levels of the BDL and sham rats (0.28 ± 0.1 vs. 0.29 ± 0.1 mU/l, respectively).

BDL reduces both the water and glycerol permeability of the hepatocyte basolateral membrane. Functional experiments of stopped-flow light scattering were performed to evaluate

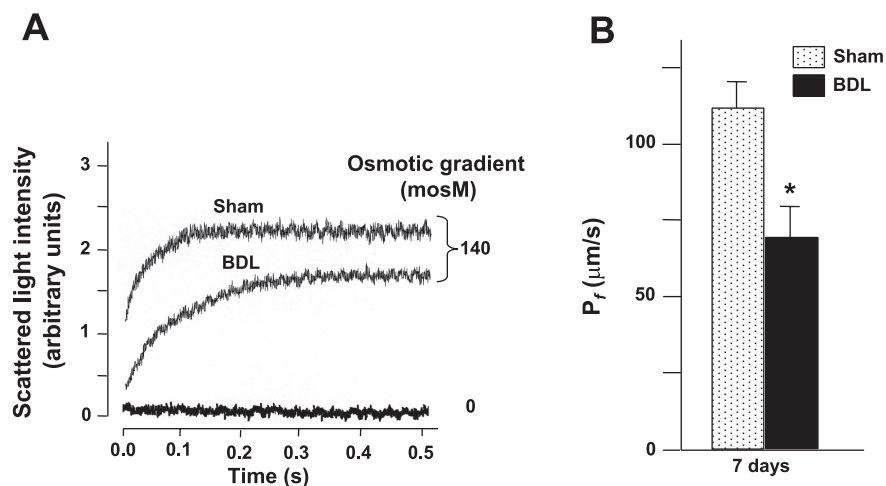


Fig. 3. Osmotic water permeability of hepatocyte basolateral membrane of sham and BDL rats after 7 days of surgery. *A*: representative tracings of stopped-flow light scattering of basolateral membrane vesicles from sham and cholestatic livers in response to a 140 mosM hypertonic mannitol gradient. No change in scattered light is observed when vesicles are mixed with isotonic buffer (absence of osmotic gradient). *B*: osmotic water permeability (P_f) after 7 days of surgery. Data are means \pm SE from 3 independent vesicle preparations. $*P < 0.05$.

whether the BDL-induced downregulation of basolateral AQP9 caused a reduction in basolateral osmotic water permeability. To do that, basolateral membrane vesicles prepared from livers of sham or 7-day BDL rats were subjected rapidly (1 ms) to a hypertonic osmotic gradient of 140 mosM and the resulting time course of vesicle shrinkage was followed from the change in scattered light. Consistent with the BDL-induced decrease of basolateral membrane AQP9 seen above and suggesting a role for AQP9 in the osmotic permeability of hepatocyte basolateral membrane, the osmotic water permeability coefficient (P_f) of the vesicles obtained from cholestatic livers was significantly lower than the one measured with the vesicles from control livers (68.3 ± 9.5 and $112 \pm 7.2 \mu\text{m/s}$, respectively; $P < 0.01$) (Fig. 3, *A* and *B*). No change in scattered light was seen when vesicles were mixed with isotonic buffer, proving the absence of mixing artifact (Fig. 3*B*).

To verify whether the BDL-induced downregulation of AQP9 was also accompanied by a reduction of the facilitated glycerol transport in hepatocyte basolateral plasma membrane, glycerol permeability was compared in basolateral membrane vesicles from livers of sham or BDL rats 7 days after surgery. Glycerol permeability was measured by light scattering following a 150 mM inwardly directed gradient of glycerol as previously described by Yang and coworkers (47). Experiments were performed at 20°C. Fig. 4*A* shows representative

light scattering data, with the slow decrease in scattered light intensity corresponding to glycerol influx into vesicles. Consistent with the osmotic water permeability studies there was significant reduction in basolateral P_{gly} coefficient in the liver of the BDL vs. sham rats (9.23 ± 1.5 and $14.6 \pm 2.6 \cdot 10^{-6} \text{ cm/s}$, respectively; $P < 0.01$) (Fig. 4*B*).

Effect of BDL on the immunocytochemical distribution of AQP9 in rat hepatocytes. Immunofluorescence and immunoperoxidase analyses with serial liver sections were performed to analyze at a subcellular level the effect of BDL on the expression and subcellular distribution of AQP9. By immunofluorescence, and in line with previous reports (7, 34, 35), livers from sham-operated rats showed AQP9 in the basolateral membrane of hepatocytes (Fig. 5*A*; arrows). No immunoreactivity was seen in the canalicular membrane (Fig. 5*A*, inset; arrowhead). No labeling was observed in normal (no surgery) liver sections by omitting the primary antibody (Fig. 5*B*). When compared with the corresponding basal conditions (*day 0*), the AQP9 immunofluorescent pattern remained unaltered in the liver of the sham-operated rats at 1, 3 and 7 days (Fig. 5, *C*, *E*, and *G*) whereas it changed markedly in the BDL liver at *day 1* and thereafter (Fig. 5, *D*, *F*, and *H*). At *day 1* of BDL (Fig. 5*D*), AQP9 was observed both over the basolateral membrane (inset; arrow) and within the intracellular compartment (double arrows). After 3 days of BDL (Fig. 5*F*),

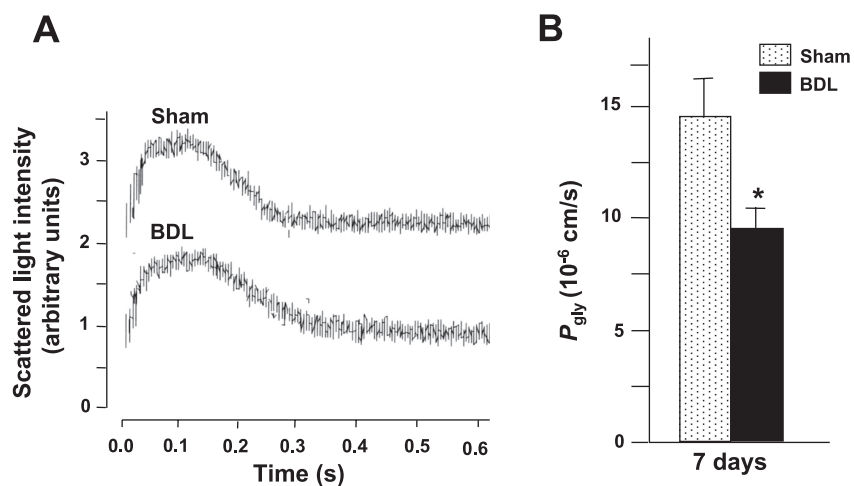


Fig. 4. Glycerol permeability of hepatocyte basolateral plasma membrane of BDL rats. *A*: representative tracings of stopped-flow light scattering of basolateral membrane vesicles from sham and BDL livers in response to a 150 mM inwardly directed gradient of glycerol at 20°C. The initial increase in light scattering results from osmotic water efflux (vesicle shrinkage), followed by a slower decrease caused by glycerol entry. *B*: glycerol permeability (P_{gly}) after 7 days of BDL and sham surgeries. Data are means \pm SE from 3 rats per each experimental condition. $*P < 0.05$.

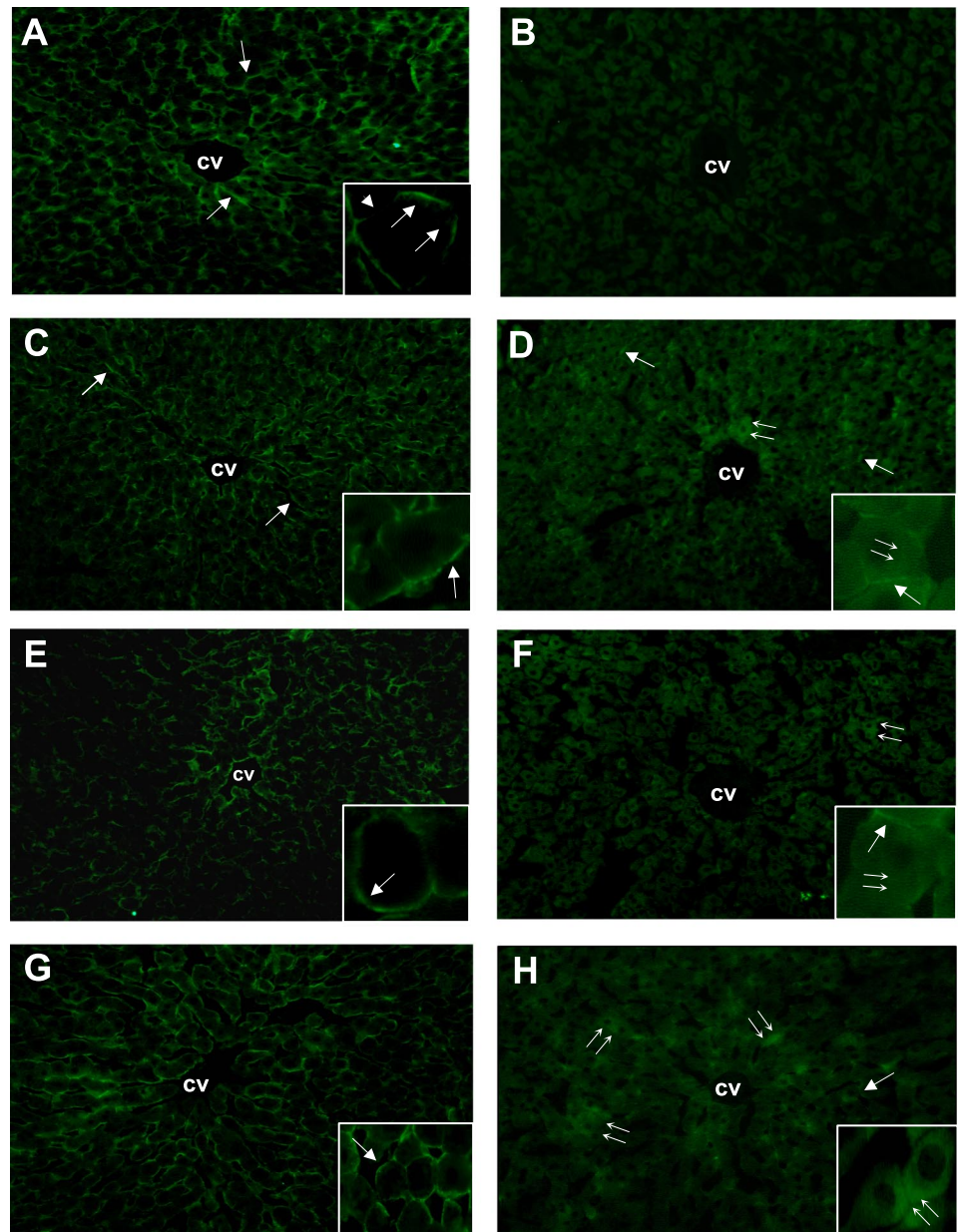


Fig. 5. Immunofluorescent distribution of AQP9 in the liver of BDL rats. *A, C, E,* and *G*: liver sections from sham-operated rats. At 0 days of BDL, AQP9 immunofluorescence is seen over the basolateral membrane of hepatocytes (*A*, arrows) and no reactivity is noted in the canalicular membrane (*A*, inset; arrowhead). Such profile of immunoreactivity is maintained in the livers of 1-, 3-, and 7-day sham rats (*C, E,* and *G*, respectively). *B*: negative control. At *day 1* of BDL (*D*), AQP9 immunoreactivity is seen both over the basolateral membrane (inset; arrow) and within the intracellular compartment (double arrows). At *day 3* of BDL (*F*), whereas the intracellular staining of AQP9 is steadily present (double arrows), the basolateral membrane labeling appears reduced both as extension and intensity (inset; arrow). At 7 days of BDL (*H*), the plasma membrane staining is very weak (single arrow) whereas extensive clouds of immunoreactivity are seen within the cytoplasmic compartment (double arrows). cv, Centrolobular vein.

the intracellular immunostaining increased (double arrows) whereas the basolateral membrane reactivity was reduced (inset; arrow). Suggesting mistrafficking of AQP9 in hepatocyte at 7-day BDL, the immunofluorescence was mostly restricted within the cytoplasmic compartment (Fig. 5D, double arrow). This pattern of distribution was confirmed by immunoperoxidase light microscopy (Fig. 6).

The altered subcellular distribution of hepatocyte AQP9 in BDL rats was also analyzed at an ultrastructural level by immunogold electron microscopy (Fig. 7). In line with the above immunocytochemical studies, cholestatic hepatocytes (*day 7* of BDL) showed predominant immunoreactivity within the cytoplasmic compartment associated with weak staining at the basolateral membrane (Fig. 7B). This pattern was significantly different from the one of the control hepatocytes where the gold particles were mostly located over the basolateral plasma membrane (Fig. 7A).

DISCUSSION

Extrahepatic cholestasis is a pathological condition caused by rapidly developing (acute) or long-term (chronic) interruption in the excretion of bile (i.e., bile solutes and water) into bile canaliculus (6). After showing impaired expression of canalicular AQP8 water channels in the liver of BDL rats (4), here we evaluated AQP9 as possible basolateral water channel contributing to bile flow dysfunction of cholestatic hepatocyte. The major finding is that extrahepatic obstruction causes strong reduction of both basolateral AQP9 and osmotic water permeability suggesting that basolateral AQP9 also functions as water channel and is pathophysiologically relevant to extrahepatic cholestasis.

There is experimental evidence indicating that rat hepatocyte basolateral osmotic water transport is AQP mediated (30). Since no other water channels are found in the rat hepatocyte

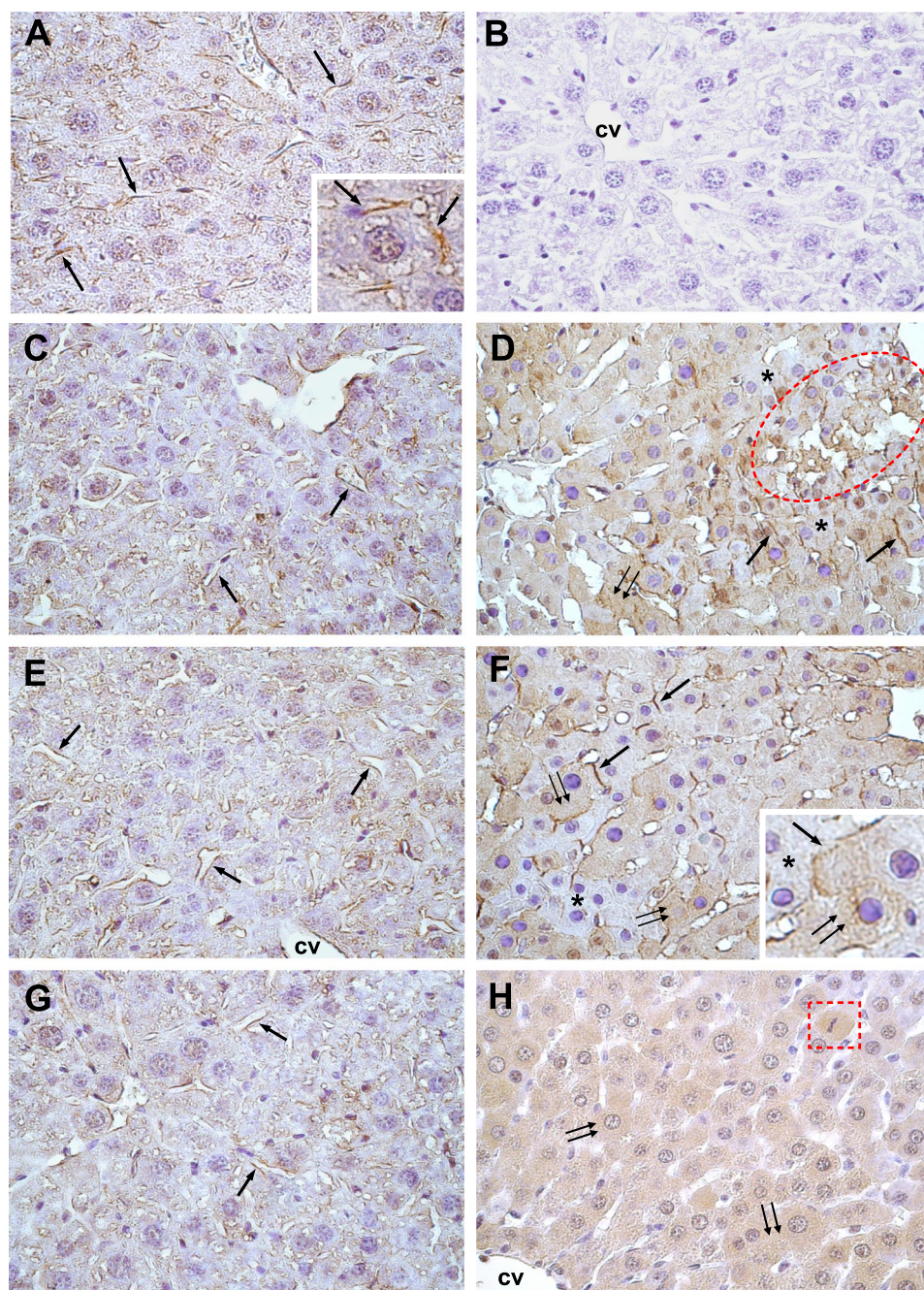


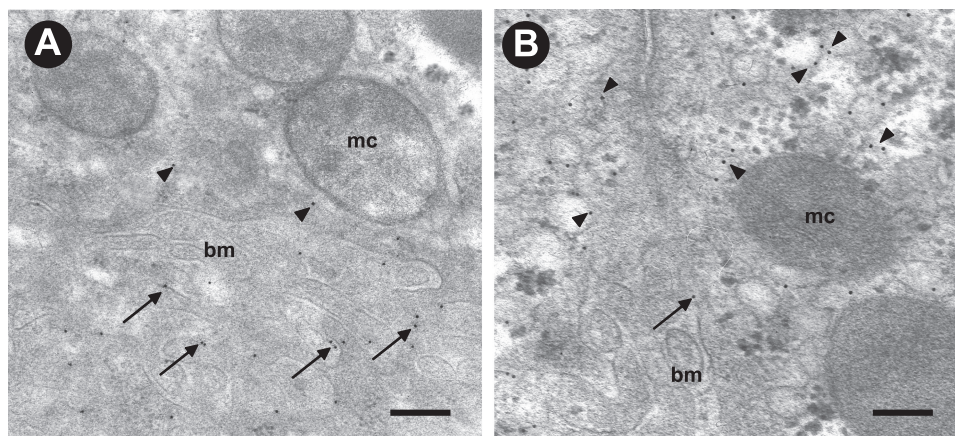
Fig. 6. Effect of bile duct ligation on the immunohistochemical distribution of AQP9 in rat hepatocytes. *A, C, E, and G*: liver sections from sham-operated rats. At *day 0*, AQP9 immunolabeling (brown staining) is seen over the basolateral membrane of hepatocytes (*A*, arrows; *inset*). Such profile of immunoreactivity is maintained in the livers of 1-, 3-, and 7-day sham rats (*C, E, and G*, respectively). *B*: negative control (absence of AQP9 antibody). *D*: *day 1* of BDL. Low AQP9 reactivity is seen over the basolateral membrane of hepatocyte (arrows). Labeling is observed over the intracellular compartment (double arrows). Areas within the hepatic acinus show hepatocytes in their way to be decomposed (red dashed circle). These areas are surrounded by hepatocytes with weak (or absent) AQP9 reactivity (asterisks). *F*: *day 3* of BDL. The labeling of the sinusoidal membrane (arrows; *inset*) is reduced as to the basal condition whereas the intracellular reactivity is increasingly evident (double arrows; *inset*). Hepatocytes with no immunoreactivity are seen within the acinus (asterisks). *H*: *day 7* of BDL. Intracellular AQP9 staining predominates in nearly all hepatocytes (double arrows). Mitotic hepatocytes with considerable intracellular staining are often observed within the acinus (red dashed square). Magnification $\times 500$ (*insets*, $\times 1,000$).

basolateral membrane (see Ref. 37 for a review), it is reasonable to hypothesize that AQP9 facilitates the sinusoidal movement of water across the hepatocyte basolateral membrane. Bile secretion by hepatocytes requires the osmotically driven transcellular transport of water (i.e., across basolateral and canalicular plasma membrane domains); thus AQP9 is expected to mediate the sinusoidal water transport during the formation of bile.

Hepatocyte AQP9 is currently known for mediating the uptake of plasma glycerol deriving from adipose lipolysis during starvation (3, 23, 38), a feature in line with our finding that the BDL-induced downregulation of liver AQP9 is also accompanied with a reduction in the P_{gly} coefficient of the hepatocyte basolateral plasma membrane (Fig. 4). Hepatocyte

AQP9 would therefore act as water or glycerol channel, depending on the physiological condition. The water channel activity of AQP9 may be relevant to primary bile formation, a function that may explain the rapid shifts of hepatocyte volume characterizing the so-called hepatocellular hydration state, an efficient mechanism of short-term control of canalicular secretion (16). The involvement of AQP9 in canalicular bile formation is also supported by the downregulation to which such AQP undergoes in the liver of BDL rat. A similar dysregulation characterizes the water channel at the canalicular side, AQP8 (4). The mechanisms involved in the defective basolateral AQP9 expression in extrahepatic cholestasis may be specific for this particular bile secretory disorder, since, as we recently reported, hepatocyte AQP9 appears unaffected in

Fig. 7. Ultrastructural localization of hepatocyte AQP9 in 7-day BDL rats by immunogold electron microscopy. **A:** hepatocyte of sham-operated rat liver. AQP9 immunogold labeling is seen at the microvilli of the basolateral plasma membrane (single arrows). Poorly appreciable staining is seen within the intracellular compartment (arrowheads). **B:** hepatocyte of BDL rat. Predominant immunolabeling is observed intracellularly (arrowheads) whereas minor staining is encountered at the basolateral membrane compartment (single arrow). mc, mitochondrion; bm, basolateral membrane; bars, 300 nm.



sepsis-associated cholestasis induced by lipopolysaccharides (26) and estrogen-induced hepatocellular cholestasis (5), two forms of intrahepatic cholestasis. The recent observation that AQP9 is downregulated at both mRNA and protein levels in the liver of neonatal (but not adult) rats treated with the synthetic estrogen diethylstilbestrol has been interpreted as due to the higher susceptibility to estrogen-induced changes characterizing newborn animals compared with their adult counterparts (45).

The observation that the 85% decrease of basolateral membrane AQP9 is associated with a 40% decrease of the basolateral membrane osmotic water permeability is valuable information in the understanding of the mechanisms of bile formation and consistent with the moderate water conductance characterizing AQP9 (3, 30). This suggests, as shown before (30), that the lipid membrane pathway may provide a nonnegligible contribution to the overall water permeability of the hepatocyte basolateral membrane. A similar explanation was given to describe the canalicular membrane water permeability (5, 26, 30). A 40% decrease of basolateral membrane osmotic water permeability may be sufficient to impair the efficient coupling between osmotic solutes and water transport during bile formation. This possibility is supported by our recent work showing that a 22% decrease of the canalicular membrane osmotic permeability is associated with a 58% decrease of canalicular bile flow (5). As seen for apical AQP8 (4), the rate of primary bile secretion may be a factor influencing the expression and distribution of AQP9 in hepatocyte. It is therefore conceivable to hypothesize that basolateral AQP9 is reduced following the impairment of the transient osmotic gradient caused by the defective sinusoidal bile salt uptake characterizing extrahepatic cholestasis (11). Since canalicular expression of AQP8, an aquaporin having a considerably higher water channel activity than AQP9, is decreased after BDL (4, 5), it is objectively not obvious to independently establish the exact importance of liver AQP9 in extrahepatic cholestasis. This difficulty may also explain why no apparent bile formation defects were seen in AQP9 knockout mice (38). Downregulation of AQP9 may be secondary to defective primary bile secretion in the light of a recent work showing normal plasma levels of alkaline phosphatase and cholesterol, two biochemical parameters of cholestasis, in AQP9-null mice (38).

Our data suggest, as previously for canalicular AQP8 in BDL rats (4), a posttranslational mechanism (e.g., increased

protein degradation as a consequence of subcellular misrouting) for basolateral AQP9 downregulation in obstructive cholestasis. Altered plasma membrane targeting is a frequent mechanism of dysregulation affecting diverse hepatocyte transporters in cholestasis, including the basolateral Na^+ /bile acid cotransporter (9, 11, 40, 41). However, a novelty of the physiological process of primary bile formation raising from this work is the fact that loss of AQP9 occurs in the context of other sinusoidal membrane proteins being targeted correctly and/or increasing in expression after BDL [i.e., the multidrug resistance-associated proteins 3, Mrp3 (44)]. Similar to canalicular AQP8 (5, 26) and AQPs expressed in cells other than hepatocytes (27, 29, 39), misrouted AQP9 may be targeted for proteolysis through the proteasome and/or lysosome system. In this scenario, a role for insulin, a hormone negatively regulating AQP9 at a gene level (3, 23), can be ruled out since both insulinemia and AQP9 transcript levels of the BDL rats did not change significantly during cholestasis.

Under the cholestasis conditions, a large amount of biliary lipids including cholesterol, bile acids, phospholipids, and bilirubin would accumulate within the hepatocyte. Indeed, the complex changes of both liver metabolism and functions with cholestasis are partly dependent on retention of hydrophobic bile salts (i.e., tauro- and glycochenodeoxycholate, major bile salts in rat bile) and reduced hepatic detoxification capacity (19, 21). In turn, this status might activate injuring pathways that might cause the decrease of antioxidant defenses including glutathione levels, stimulate glutathione efflux from hepatocytes (15), and induce necrosis by activating the mitochondrial membrane permeability transition (14). Of note, maintenance of intracellular glutathione levels is important also for the regulation of bile formation (13). These factors worsen hepatic oxidative stress, decrease glutathione stores, and impair the detoxification defenses (22, 43). Indeed, in a recent study, we could show that in the liver, ongoing cholestasis was associated with early oxidative changes (36). Further investigation is needed to evaluate whether these factors influence the expression and distribution of AQP9 in hepatocytes as well.

Because impaired hepatic fatty acid metabolism has been shown in either long- (21) and short-term (24) extrahepatic cholestasis it is conceivable to think that dysfunctional expression of hepatic AQP9 induced by BDL may influence fatty acid metabolism in the liver. Although this was not the primary aim of our study we believe unlikely a direct involvement of AQP9

in triglyceride synthesis since 1) increased plasma triglyceride levels are found in rats with BDL, suggesting increased export of esterified fatty acids (20), and 2) plasma levels of glycerol and triglycerides are markedly increased in AQP9-null mice (38).

In conclusion, this work finds that hepatocyte basolateral AQP9 protein is downregulated in obstructive extrahepatic cholestasis. Such reduction is associated with a considerable decrease of the basolateral membrane osmotic water permeability. As expected, a decrease of the basolateral glycerol permeability is also observed. Besides serving as glycerol facilitator, hepatocyte AQP9 may also function as a water channel in bile formation and secretion. Because hepatic AQP8 and AQP9 are both downregulated following BDL it is conceivable to hypothesize that a defective expression of aquaporin water channels contributes to primary bile secretory dysfunction in the cholestatic liver. Of note, the identification of novel pharmacological approaches can be speculated, in which biliary epithelia are the primary target cell in patients with cholestatic diseases.

ACKNOWLEDGMENTS

The authors are grateful to Michele Persichella for skillful technical assistance.

GRANTS

This work was supported by grants PRIN-Cofin 2006 from MiUR Ministero dell'Università e della Ricerca (G. Calamita, P. Portincasa); Fondi Ateneo Ricerca Scientifica from the University of Bari, Italy (G. Calamita, M. Svelto, P. Portincasa); and PICT 05-31670 from Agencia Nacional de Promoción Científica y Tecnológica (R. A. Marinelli).

REFERENCES

- Calamita G, Ferri D, Gena P, Liquori GE, Cavalier A, Thomas D, Svelto M. The inner mitochondrial membrane has aquaporin-8 water channels and is highly permeable to water. *J Biol Chem* 280: 17149–17153, 2005.
- Calamita G, Mazzone A, Bizzoca A, Cavalier A, Cassano G, Thomas D, Svelto M. Expression and immunolocalization of the aquaporin-8 water channel in rat gastrointestinal tract. *Eur J Cell Biol* 80: 711–719, 2001.
- Carbrey JM, Gorelick-Feldman DA, Kozono D, Praetorius J, Nielsen S, Agre P. Aquaglyceroporin AQP9: solute permeation and metabolic control of expression in liver. *Proc Natl Acad Sci USA* 100: 2945–2950, 2003.
- Carreras FI, Gradilone SA, Mazzone A, Garcia F, Huang BQ, Ochoa JE, Tietz PS, Larusso NF, Calamita G, Marinelli RA. Rat hepatocyte aquaporin-8 water channels are down-regulated in extrahepatic cholestasis. *Hepatology* 37: 1026–1033, 2003.
- Carreras FI, Lehmann GL, Ferri D, Tioni MF, Calamita G, Marinelli RA. Defective hepatocyte aquaporin-8 expression and reduced canalicular membrane water permeability in estrogen-induced cholestasis. *Am J Physiol Gastrointest Liver Physiol* 292: G905–G912, 2007.
- Elferink RO. Cholestasis. *Gut* 52, Suppl 2: ii42–ii48, 2003.
- Elkjaer M, Vajda Z, Nejsum LN, Kwon T, Jensen UB, Amiry-Moghaddam M, Frokiaer J, Nielsen S. Immunolocalization of AQP9 in liver, epididymis, testis, spleen, and brain. *Biochem Biophys Res Commun* 276: 1118–1128, 2000.
- Ferri D, Mazzone A, Liquori GE, Cassano G, Svelto M, Calamita G. Ontogeny, distribution, and possible functional implications of an unusual aquaporin, AQP8, in mouse liver. *Hepatology* 38: 947–957, 2003.
- Fricker G, Landmann L, Meier PJ. Extrahepatic obstructive cholestasis reverses the bile salt secretory polarity of rat hepatocytes. *J Clin Invest* 84: 876–885, 1989.
- Garcia F, Kierbel A, Larocca MC, Gradilone SA, Splinter P, LaRusso NF, Marinelli RA. The water channel aquaporin-8 is mainly intracellular in rat hepatocytes, and its plasma membrane insertion is stimulated by cyclic AMP. *J Biol Chem* 276: 12147–12152, 2001.
- Gartung C, Ananthanarayanan M, Rahman MA, Schuele S, Nundy S, Soroka CJ, Stolz A, Suchy FJ, Boyer JL. Down-regulation of expression and function of the rat liver Na⁺/bile acid cotransporter in extrahepatic cholestasis. *Gastroenterology* 110: 199–209, 1996.
- Gorelick DA, Praetorius J, Tsunenari T, Nielsen S, Agre P. Aquaporin-11: a channel protein lacking apparent transport function expressed in brain. *BMC Biochem* 7: 14, 2006.
- Grattagliano I, Portincasa P, Palmieri VO, Palasciano G. Contribution of canalicular glutathione efflux to bile formation. From cholestasis associated alterations to pharmacological intervention to modify bile flow. *Curr Drug Targets Immune Endocr Metabol Disord* 5: 153–161, 2005.
- Guldutuna S, Zimmer G, Leuschner M, Bhatti S, Elze A, Deisinger B, Hofmann M, Leuschner U. The effect of bile salts and calcium on isolated rat liver mitochondria. *Biochim Biophys Acta* 1453: 396–406, 1999.
- Gumprich E, Devereaux MW, Dahl RH, Sokol RJ. Glutathione status of isolated rat hepatocytes affects bile acid-induced cellular necrosis but not apoptosis. *Toxicol Appl Pharmacol* 164: 102–111, 2000.
- Haussinger D, Schmitt M, Weiergraber O, Kubitz R. Short-term regulation of canalicular transport. *Semin Liver Dis* 20: 307–321, 2000.
- Huebert RC, Splinter PL, Garcia F, Marinelli RA, LaRusso NF. Expression and localization of aquaporin water channels in rat hepatocytes. Evidence for a role in canalicular bile secretion. *J Biol Chem* 277: 22710–22717, 2002.
- King LS, Kozono D, Agre P. From structure to disease: the evolving tale of aquaporin biology. *Nat Rev Mol Cell Biol* 5: 687–698, 2004.
- Krahenbuhl S. Alterations in mitochondrial function and morphology in chronic liver disease: pathogenesis and potential for therapeutic intervention. *Pharmacol Ther* 60: 1–38, 1993.
- Krahenbuhl S, Brass EP. Fuel homeostasis and carnitine metabolism in rats with secondary biliary cirrhosis. *Hepatology* 14: 927–934, 1991.
- Krahenbuhl S, Fischer S, Talos C, Reichen J. Ursodeoxycholate protects oxidative mitochondrial metabolism from bile acid toxicity: dose-response study in isolated rat liver mitochondria. *Hepatology* 20: 1595–1601, 1994.
- Krahenbuhl S, Talos C, Lauterburg BH, Reichen J. Reduced antioxidant capacity in liver mitochondria from bile duct ligated rats. *Hepatology* 22: 607–612, 1995.
- Kuriyama H, Shimomura I, Kishida K, Kondo H, Furuyama N, Nishizawa H, Maeda N, Matsuda M, Nagaretani H, Kihara S, Nakamura T, Tochino Y, Funahashi T, Matsuzawa Y. Coordinated regulation of fat-specific and liver-specific glycerol channels, aquaporin adipose and aquaporin 9. *Diabetes* 51: 2915–2921, 2002.
- Lang C, Schafer M, Serra D, Hegardt F, Krahenbuhl L, Krahenbuhl S. Impaired hepatic fatty acid oxidation in rats with short-term cholestasis: characterization and mechanism. *J Lipid Res* 42: 22–30, 2001.
- Lee J, Boyer JL. Molecular alterations in hepatocyte transport mechanisms in acquired cholestatic liver disorders. *Semin Liver Dis* 20: 373–384, 2000.
- Lehmann GL, Carreras FI, Soria LR, Gradilone SA, Marinelli RA. LPS induces the TNF α -mediated downregulation of rat liver aquaporin-8: role in sepsis-associated cholestasis. *Am J Physiol Gastrointest Liver Physiol* 294: G567–G575, 2008.
- Leitch V, Agre P, King LS. Altered ubiquitination and stability of aquaporin-1 in hypertonic stress. *Proc Natl Acad Sci USA* 98: 2894–2898, 2001.
- Lowry OH, Rosebrough NJ, Farr AL, Randall RJ. Protein measurement with the Folin phenol reagent. *J Biol Chem* 193: 265–275, 1951.
- Madrid R, Le Maout S, Barrault MB, Janvier K, Benichou S, Merot J. Polarized trafficking and surface expression of the AQP4 water channel are coordinated by serial and regulated interactions with different clathrin-adaptor complexes. *EMBO J* 20: 7008–7021, 2001.
- Marinelli RA, Tietz PS, Caride AJ, Huang BQ, LaRusso NF. Water transporting properties of hepatocyte basolateral and canalicular plasma membrane domains. *J Biol Chem* 278: 43157–43162, 2003.
- Masyuk AI, LaRusso NF. Aquaporins in the hepatobiliary system. *Hepatology* 43: S75–81, 2006.
- Meier PJ, Sztul ES, Reuben A, Boyer JL. Structural and functional polarity of canalicular and basolateral plasma membrane vesicles isolated in high yield from rat liver. *J Cell Biol* 98: 991–1000, 1984.
- Morishita Y, Matsuzaki T, Hara-chikuma M, Andoo A, Shimono M, Matsuki A, Kobayashi K, Ikeda M, Yamamoto T, Verkman A, Kusano E, Ookawara S, Takata K, Sasaki S, Ishibashi K. Disruption of aquaporin-11 produces polycystic kidneys following vacuolization of the proximal tubule. *Mol Cell Biol* 25: 7770–7779, 2005.
- Nicchia GP, Frigeri A, Nico B, Ribatti D, Svelto M. Tissue distribution and membrane localization of aquaporin-9 water channel: evidence for sex-linked differences in liver. *J Histochem Cytochem* 49: 1547–1556, 2001.

35. Nihei K, Koyama Y, Tani T, Yaoita E, Ohshiro K, Adhikary LP, Kurosaki I, Shirai Y, Hatakeyama K, Yamamoto T. Immunolocalization of aquaporin-9 in rat hepatocytes and Leydig cells. *Arch Histol Cytol* 64: 81–88, 2001.
36. Portincasa P, Grattagliano I, Testini M, Caruso ML, Wang DQ, Moschetta A, Calamita G, Vacca M, Valentini AM, Renna G, Lissidini G, Palasciano G. Parallel intestinal and liver injury during early cholestasis in the rat: modulation by bile salts and antioxidants. *Free Radic Biol Med* 42: 1381–1391, 2007.
37. Portincasa P, Palasciano G, Svelto M, Calamita G. Aquaporins in the hepatobiliary tract. Which, where and what they do in health and disease. *Eur J Clin Invest* 38: 1–10, 2008.
38. Rojek AM, Skowronski MT, Fuchtbauer EM, Fuchtbauer AC, Fenton RA, Agre P, Frokiaer J, Nielsen S. Defective glycerol metabolism in aquaporin 9 (AQP9) knockout mice. *Proc Natl Acad Sci USA* 104: 3609–3614, 2007.
39. Sidhaye V, Hoffert JD, King LS. cAMP has distinct acute and chronic effects on aquaporin-5 in lung epithelial cells. *J Biol Chem* 280: 3590–3596, 2005.
40. Song JY, Van Noorden CJ, Frederiks WM. The involvement of altered vesicle transport in redistribution of Ca^{2+} , Mg^{2+} -ATPase in cholestatic rat liver. *Histochem J* 30: 909–916, 1998.
41. Stieger B, Meier PJ, Landmann L. Effect of obstructive cholestasis on membrane traffic and domain-specific expression of plasma membrane proteins in rat liver parenchymal cells. *Hepatology* 20: 201–212, 1994.
42. Van Heeswijk MP, van Os CH. Osmotic water permeabilities of brush border and basolateral membrane vesicles from rat renal cortex and small intestine. *J Membr Biol* 92: 183–193, 1986.
43. Vendemiale G, Grattagliano I, Lupo L, Memeo V, Altomare E. Hepatic oxidative alterations in patients with extra-hepatic cholestasis. Effect of surgical drainage. *J Hepatol* 37: 601–605, 2002.
44. Villanueva SS, Ruiz ML, Ghanem CI, Luquita MG, Catania VA, Mottino AD. Hepatic synthesis and urinary elimination of acetaminophen glucuronide are exacerbated in bile duct-ligated rats. *Drug Metab Dispos* 36: 475–480, 2008.
45. Wellejus A, Jensen HE, Loft S, Jonassen TE. Expression of aquaporin 9 in rat liver and efferent ducts of the male reproductive system after neonatal diethylstilbestrol exposure. *J Histochem Cytochem* 56: 425–432, 2008.
46. Yakata K, Hiroaki Y, Ishibashi K, Sohara E, Sasaki S, Mitsuoka K, Fujiyoshi Y. Aquaporin-11 containing a divergent NPA motif has normal water channel activity. *Biochim Biophys Acta* 1768: 688–693, 2007.
47. Yang B, Zhao D, Verkman AS. Evidence against functionally significant aquaporin expression in mitochondria. *J Biol Chem* 281: 16202–16206, 2006.

